Available online at www.easdprocedia.org
EASD Procedia EURODYN (2020) 2893-2908

EASD Procedia

EURODYN 2020
XI International Conference on Structural Dynamics
M. Papadrakakis, M. Fragiadakis, C. Papadimitriou (eds.)
Athens, Greece, 23–26 November 2020

INCREMENTAL DYNAMIC ANALYSES OF BRIDGE PYLONS WITH CONSIDERATION OF THE EFFECT OF SURFACE WAVES

Charisis T. Chatzigogos[1] and Kristel C. Meza Fajardo[2]

[1] Géodynamique & Structure
Montrouge, France
e-mail: charisis.chatzigogos@geodynamique.com

[2] Bureau de Recherches Géologiques et Mineurs
Orléans, France
k.mezafajardo@brgm.fr

Keywords: bridge pylon design, surface waves, nonlinear soil-structure interaction, surrogate models, incremental dynamic analyses

Abstract. *The impact of surface waves on long-period structures remains among the less well understood aspects in the earthquake-resistant design of civil structures. Surface waves are typically characterized by rich low-frequency content and long durations and accordingly they can be particularly damaging for long-period structures, such as high-rise buildings, bridge pylons, liquid storage tanks, telecommunication masts etc. It is understood that an insufficient seismic design may be obtained for this class of structures if the effect of surface waves is not taken into account in the definition of earthquake loading. The present paper proposes a concise surrogate mechanical model for the study of the seismic nonlinear response of bridge pylons with and without the consideration of the effect of surface waves on dynamic response. The model is fully parametrizable based on a reduced number of dimensionless parameters that allow generating a large set of different structural and foundation configurations. The model couples a multi-fiber beam model for the bridge pylon with a nonlinear macroelement for the pylon foundation, accounting for sliding, uplifting and partial or full loss of bearing capacity in the foundation soil. This coupled pylon-foundation model is subjected to three cases of record sets for performing Incremental Dynamic Analyses (IDA), in which the records may preserve or not the surface wave components in the horizontal and rotational degrees-of-freedom of the incident motion. The IDA methodology is exploited for presenting in a synthetic manner the overall dynamic response for two characteristic bridge pylon designs and for highlighting the situations in which the non-consideration of surface waves may indeed lead to an insufficient design.*

Peer-review under responsibility of the Organizing Committee of EURODYN 2020.
doi: 10.47964/1120.9237.19409

1 INTRODUCTION

A common assumption in normative seismic studies of civil structures is to establish ground motions (to be used as incident excitations at the foundation level) via 1D site response analyses, in which the vertical propagation of shear waves is studied along an idealized soil column (1D model). Despite its efficiency, this approach wipes out the effects of real 3D topography of the subsoil and, in particular, the eventual presence of surface waves (Rayleigh waves / Love waves). Surface waves are typically generated in geological settings such as sedimentary basins and are characterized by rich low-frequency content and long durations. For example, presence of Rayleigh waves in the incident motion will lead to an increase in horizontal spectral accelerations (translational component) in the low-frequency range and also will generate a rotational component that cannot be obtained via 1D site response analyses.

Notwithstanding the ubiquitous principle, already anticipated by Biot [1] in the 1930's (*cf*. Trifunac [2]) that under favorable conditions (long waves), rotational seismic motions are small and can be neglected, several recent strong earthquakes (*e.g*. Chi-Chi 1999, Chuetsu 2004, El Mayor 2010, Tohoku 2011) have revealed significant rotational motions related to the passage of surface waves. These motions can be detrimental for long-period structures such as high-rise buildings, bridge pylons and liquid storage tanks, to name the most important ones.

Available studies for assessing the impact of surface waves on long-period structures are rather scarce. In two recent papers [3], [4], Meza & Papageorgiou have studied the effect of surface waves on the response of tall buildings and have shown that Rayleigh waves can increase the damage levels in such structures because of period elongation due to nonlinear response, extended shaking duration and risk of resonance. Concerning the effect of surface waves on bridge pylons, Chatzigogos *et al*. [5] have recently proposed a simplified surrogate model with consideration of nonlinear response in the pylon and/or in the foundation. The model is used for studying different soil-pylon configurations and for quantifying the increase in seismic demand (with respect to several performance criteria) due to the consideration of surface waves.

The present paper aims to extend the initial results obtained by Chatzigogos *et al*. [5] by probing -in a more systematic way- the impact of surface waves on nonlinear response of selected soil-pylon configurations via the technique of Incremental Dynamic Analysis (IDA) [6]. IDA is by now a well-established method for gaining insight into nonlinear seismic response for increasing levels of shaking. The studied bridge pylons are subjected to various records of increasing intensity and this allows plotting Damage Measures (DM) of interest as functions of appropriately selected seismic Intensity Measures (IM). The analyses are performed with and without consideration of the surface wave component of the considered records and this allows quantifying the additional distress provoked by the incidence of surface waves.

2 SURROGATE MODEL FOR BRIDGE PYLONS

2.1 General principles

In the following, we concentrate on the study of bridge pylons as shown on Figure 1. The surrogate model proposed by Chatzigogos *et al*. [5] will be used hereafter for studying the response of two characteristic pylon configurations with the IDA methodology. The model is intended for studying the transverse dynamic response of single-branch pylons (piers) and it is formulated in 2D kinematics. The pier supports at its top a part of the bridge deck and the deck-pier connection is concretized via a local spring-dashpot element. The pier foundation is a shallow footing resting at the ground surface (the footing embedment is neglected). Basic features of the surrogate model are the following:

- *Consideration of full nonlinear pier response in bending*. This is achieved by discretizing the pier into 2-noded multi-fiber beam elements. The cross-section of the pier is equally discretized into a number of fibers that are assigned an appropriate 1D nonlinear law. For the application presented hereafter, the nonlinear model for the fibers will be a simple elastoplastic law, with initial elastic stiffness E_p, yield stress f_y and post-elastic stiffness $E'_p = \alpha_k E_p$ (α_k: proportionality constant). In terms of global behavior, parameters E_p and f_y give rise to yield bending moment $M_{p,y}$ and yield curvature κ_y of the pier section.
- *Nonlinear response at the foundation level*. This is achieved via a dedicated nonlinear foundation macroelement following Chatzigogos *et al*. [7]. This model is briefly presented in §2.3.
- *Translational and rotational seismic excitation*. The excitation is introduced as imposed displacement to a control point at the base of the model. Following [5], three scenarios will be studied hereafter: a) only horizontal excitation without surface wave effect, b) only horizontal excitation, enriched with surface wave effect and c) horizontal and rotational excitations with full consideration of surface wave effects. For simplicity, vertical component of seismic motion is neglected in the presented analyses.
- *Solution in time domain*. The resulting dynamic equilibrium equation is integrated in time domain using an unconditionally stable Newmark scheme under the assumption of small displacements. Calculations are run in the open-source FEM platform Code_ASTER [8].

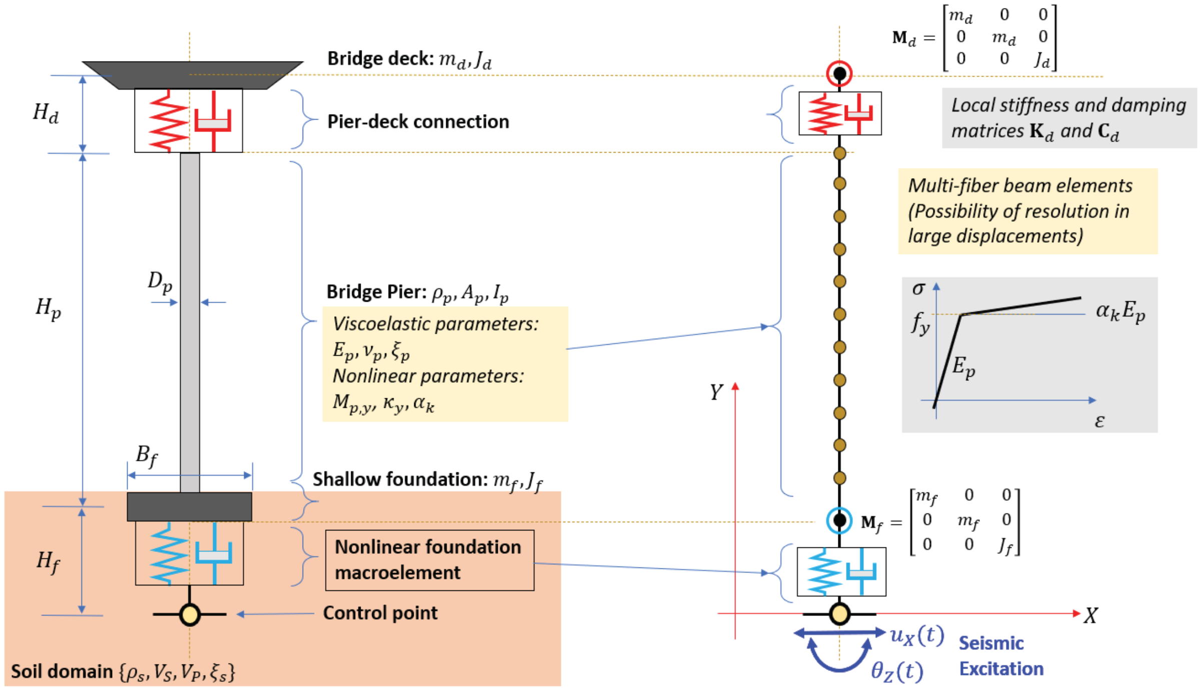

Figure 1: Surrogate model for studying the effects of surface waves on bridge pylons.

2.2 Geometric and mechanical characterization

The proposed surrogate model is intended for efficiently generating a large number of different pylon-foundation configurations, in the search for those cases that are particularly vulnerable in the incidence of surface waves. Each instance of the surrogate model can accordingly be obtained via a set of geometric and mechanical parameters that are organized into vector **a** that groups a limited number of dimensional parameters and into vector **b** that groups all other governing quantities that are either dimensionless or expressed as normalized parameters. In the definition of governing model parameters, we use subscripts p, d, f and s to designate respectively the pier, the deck, the foundation and the soil. Normalized parameters are designated with a tilde (~).

The vector of dimensional parameters reads:

$$\mathbf{a}^{\mathrm{T}} = \{H_p, m_p, A_p, E_p, T_p, M_{p,y}, W_{\mathrm{tot}}\} \tag{1}$$

with the following definitions:

- H_p : height of bridge pier
- m_p : mass of bridge pier
- A_p: cross-sectional area of pier (considered uniform in the entire height)
- E_p : Young's modulus of bridge pier (initial elastic stiffness)
- T_p : fundamental period of vibration of the pier considering fixed-base conditions
- $M_{p,y}$: yield bending moment of pier section
- $W_{\mathrm{tot}} = g(m_p + m_d + m_f)$: total weight of the structure

The definition of the surrogate model is completed by 17 additional parameters that are either dimensionless or are normalized and are grouped in vector **b**, which reads:

$$\mathbf{b}^{\mathrm{T}} = \{\widetilde{H}_d, \widetilde{D}_p, \widetilde{H}_f, \widetilde{B}_f, \widetilde{m}_d, \widetilde{m}_f, \tilde{J}_d, \tilde{J}_f, \xi_p, \xi_s, \nu_p, \nu_s, \tilde{\rho}_s, \tilde{V}_S, \widetilde{N}_{f,\max}, \tilde{V}_{f,\max}, \widetilde{M}_{f,\max}\} \tag{2}$$

with the following definitions:

- $\widetilde{H}_d = H_d/H_p$: normalized height of the bridge deck (form pier top to the center of gravity of bridge deck, *cf.* Figure 1)
- $\widetilde{D}_p = D_p/H_p$: normalized bridge pier diameter (or equivalent diameter for non-circular pier sections)
- $\widetilde{H}_f = H_f/H_p$: normalized foundation height (from pier base to the center of gravity of bridge footing)
- $\widetilde{B}_f = B_f/H_p$: normalized characteristic footing dimension
- $\widetilde{m}_d = m_d/m_p$: normalized mass of bridge deck supported by the pier
- $\widetilde{m}_f = m_f/m_p$: normalized mass of bridge foundation
- $\tilde{J}_d = J_d/m_p H_p^2$: normalized rotational inertia of bridge deck
- $\tilde{J}_f = J_f/m_p H_p^2$: normalized rotational inertia of foundation
- ξ_p : critical damping ratio for the bridge pier (in the linear viscoelastic range)
- ξ_s : critical material damping ratio in the soil (in the linear viscoelastic range)
- ν_p : Poisson's ratio for the bridge pier
- ν_s : Poisson's ratio in the soil
- $\tilde{\rho}_s = \rho_s/(\frac{m_p}{A_p H_p})$: normalized soil mass density
- $\tilde{V}_S = V_S/(\frac{H_p}{T_p})$: normalized shear wave velocity (rigidity contrast between soil and structure)
- $\widetilde{N}_{f,\max} = N_{f,\max}/W_{\mathrm{tot}}$: maximum centered force supported by the foundation
- $\tilde{V}_{f,\max} = V_{f,\max}/W_{\mathrm{tot}}$: maximum horizontal force supported by the foundation
- $\widetilde{M}_{f,\max} = M_{f,\max}/M_{p,y}$: maximum overturning moment supported by the foundation

The above definitions for the pylon foundation imply that it is possible to determine dynamic impedance terms (computed at the fundamental SSI frequency of the pylon) assuming equivalent foundation dimension B_f and the homogenized linear viscoelastic soil domain with parameters $\{\rho_s, \nu_s, V_S, \xi_s\}$. For a surface footing (anticipating negligible off-diagonal impedance terms) and 2D kinematics, three stiffness terms $\{K_{NN}, K_{VV}, K_{MM}\}$ and the corresponding damping terms $\{C_{NN}, C_{VV}, C_{MM}\}$ are obtained.

2.3 Nonlinear foundation macroelement

An important feature of the proposed model is the use of a dedicated macroelement for description of nonlinear response at foundation level. The implemented foundation macroelement follows the formulation proposed by Chatzigogos *et al*. [7]. The foundation macroelement is an advanced link element that is placed at the base of the model and aims at reproducing nonlinear foundation response under earthquake action. The macroelement provides a phenomenological constitutive law for relating the increment of foundation displacements $\dot{\mathbf{u}}_f$ to the corresponding increment of work-conjugate force parameters $\dot{\mathbf{Q}}$. For obtaining the macroelement constitutive law, total displacement increment is decomposed into the linear elastic counterpart $\dot{\mathbf{u}}_{\mathrm{lin}}$ that is computed from impedance terms, and counterparts for three independent nonlinear mechanisms: sliding ($\dot{\mathbf{u}}_{\mathrm{sl}}$), foundation uplifting ($\dot{\mathbf{u}}_{\mathrm{up}}$) and soil plasticity ($\dot{\mathbf{u}}_{\mathrm{sp}}$). Total displacement increment $\dot{\mathbf{u}}_f$ thus reads:

$$\dot{\mathbf{u}}_f = \dot{\mathbf{u}}_{\mathrm{lin}} + \dot{\mathbf{u}}_{\mathrm{up}} + \dot{\mathbf{u}}_{\mathrm{sl}} + \dot{\mathbf{u}}_{\mathrm{sp}} \tag{3}$$

Each nonlinear mechanism is described independently by an appropriate model. In particular, sliding mechanism is described by the standard Coulomb friction criterion with a non-associative flow rule. Soil plasticity is described by a bounding surface hypoplastic formulation [10] that can easily be adapted to soil behavior (cohesive, frictional or combination of the two). Finally, uplift mechanism is described by a phenomenological nonlinear elastic model that respects the perfect reversibility of this mechanism and depends solely on foundation geometry. Coupling between nonlinear mechanisms is achieved by solving simultaneously the nonlinear equations of each mechanism (with only minor adjustments in the formulation of each mechanism) for the same force increment. A detailed presentation of the foundation macroelement model implemented in this study is provided in references [5] and [7].

3 STUDIED CONFIGURATIONS

The analyses presented hereafter are performed for two pylon configurations corresponding to two types of seismic design philosophy for the foundation. The first configuration corresponds to what would be a conventional design, in which the foundation is designed with an over-strength (in terms of overturning moment) with respect to the bending moment capacity at the pylon base. Such a design implies that damage will be concentrated at the base of the bridge pylon, while the foundation should exhibit a quasi-linear response.

In the second configuration, the foundation dimension is reduced, inviting for development of nonlinear response at the foundation level (via activation of sliding, uplifting and soil plasticity mechanisms). Such an "inversion" in conventional capacity-design of interacting foundation-superstructure systems has been proposed by many researchers (*e.g.* [12]) as a viable means of seismic protection of structures with an affordable scheme for foundation design. The price to pay is the irreversible foundation response and the pronounced displacements at the top of the pylon (due to uplifting and high foundation rotations) that must be shown to remain in acceptable limits.

Table 1 presents the geometric and mechanical parameters that define the two studied configurations. Given that the pier height is $H_p = 30\text{m}$, the configurations are designated “P30-Large” or simply P30L and “P30-Small” or simply P30S.

P30L exhibits a foundation with characteristic dimension $B_f = 11.0\text{m}$. For P30S, $B_f = 7.0\text{m}$. Table 1 provides the dimensional (vector **a**) and dimensionless parameters (vector **b**) defining the studied configurations. For convenience, Table 1 also provides the dimensional parameters corresponding to vector **b**.

	PHYSICAL QUANTITY	SYMBOL	UNIT	P30 (LARGE)	P30 (SMALL)				
Dimensional	Column height	H_p	[m]	30.0	30.0				
Dimensional	Total mass of the pier	m_p	[kt]	0.530	0.530				
Dimensional	Pier cross-sectional area	A_p	[m²]	7.1	7.1				
Dimensional	Young modulus of pier	E_p	[MPa]	30000	30000				
Dimensional	Fundamental period (fixed-base conditions)	T_p	[sec]	2.036	2.036				
Dimensional	Yield moment of pier section	$M_{p,y}$	[MNm]	43.0	43.0	Dimensional			
Dimensional	Total weight of bridge pier	W_{tot}	[MN]	22.91	19.38	SYMBOL	UNIT	P30 (LARGE)	P30 (SMALL)
Dimensionless / Normalized	Pier-deck connection height (normalized)	$\tilde{H}_d$	[-]	0.0	0.0	H_d	[m]	0.0	0.0
Dimensionless / Normalized	Pier section diameter (normalized)	$\tilde{D}_p$	[-]	0.1000	0.1000	D_p	[m]	3.0	3.0
Dimensionless / Normalized	Foundation height (normalized)	$\tilde{H}_f$	[-]	0.0667	0.0667	H_f	[m]	2.0	2.0
Dimensionless / Normalized	Foundation characteristic dimension (normalized)	$\tilde{B}_f$	[-]	0.3667	0.2333	B_f	[m]	11.0	7.0
Dimensionless / Normalized	Mass of the deck (normalized)	$\tilde{m}_d$	[-]	2.2642	2.2642	m_d	[kt]	1.2	1.2
Dimensionless / Normalized	Mass of the foundation (normalized)	$\tilde{m}_f$	[-]	1.1415	0.4623	m_f	[kt]	0.6	0.2
Dimensionless / Normalized	Moment of inertia of the deck (normalized)	$\tilde{J}_d$	[-]	0.0491	0.0491	J_d	[ktm²]	23.4	23.4
Dimensionless / Normalized	Moment of inertia of the foundation (normalized)	$\tilde{J}_f$	[-]	4.334E-04	1.730E-04	J_f	[ktm²]	0.207	0.083
Dimensionless / Normalized	Basic damping ratio of pier	ξ_p	[%]	5.0	5.0	ξ_p	[%]	5.0	5.0
Dimensionless / Normalized	Basic damping ratio of soil	ξ_s	[%]	5.0	5.0	ξ_s	[%]	5.0	5.0
Dimensionless / Normalized	Poisson's ratio of pier	ν_p	[-]	0.2	0.2	ν_p	[-]	0.2	0.2
Dimensionless / Normalized	Soil Poisson's ratio	ν_s	[-]	0.3	0.3	ν_s	[-]	0.3	0.3
Dimensionless / Normalized	Soil mass density (normalized)	$\tilde{\rho}_s$	[kt/m³]	0.643	0.643	ρ_s	[kt/m³]	0.0016	0.0016
Dimensionless / Normalized	Soil shear wave velocity (effective) (normalized)	$\tilde{V}_S$	[m/s]	17.29	17.29	V_S	[m/s]	254.8	254.8
Dimensionless / Normalized	Maximum centered vertical force at the foundation (normalized)	$\tilde{N}_{f,\max}$	[MN]	4.84	2.35	$N_{f,\max}$	[MN]	110.81	45.5
Dimensionless / Normalized	Maximum horizontal force at the foundation (normalized)	$\tilde{V}_{f,\max}$	[MN]	0.79	0.38	$V_{f,\max}$	[MN]	18.15	7.4
Dimensionless / Normalized	Maximum overturning moment at the foundation (normalized)	$\tilde{M}_{f,\max}$	[MN]	3.11	0.80	$M_{f,\max}$	[MNm]	133.77	34.5

Table 1: Geometric and mechanical parameters of studied bridge pier configurations.

Quantity	Symbol	Unit	P30 (LARGE)	P30 (SMALL)
Yield curvature of pier section	$\kappa_{p,y}$	[1/m]	0.00036	0.00036
Equivalent yield stress of pier fibers	f_y	[MPa]	16.22	16.22
Hardening parameter for pier fibers	α_k	[MPa]	0.001	0.001
Fundamental period of system with SSI	T_{SSI}	[sec]	2.167	2.506
Soil Young's modulus (effective)	E_s	[MPa]	270.00	270.00
Soil shear modulus (effective)	G_s	[MPa]	103.85	103.85
Soil P-wave velocity (effective)	V_P	[m/s]	476.60	476.60
Lysmer's analog velocity	V_{La}	[m/s]	393.88	393.88
Soil layer depth	d_s	[m]	25.00	25.00
Soil cohesion	c_u	[MPa]	0.150	0.15

(a)

PARAMETER DESCRIPTION	SYMBOL	UNIT	P30 (LARGE)	P30 (SMALL)
Footing dimension	B_f	[m]	11.00	7.00
Maximum centered vertical force	$N_{f,\max}$	[MN]	110.81	45.52
Maximum horizontal force	$V_{f,\max}$	[MN]	18.15	7.35
Maximum overturning moment	$M_{f,\max}$	[MNm]	133.77	34.47
Bounding surface parameter ψ	ψ	[-]	0.16	0.16
Bounding surface parameter ξ	χ	[-]	0.11	0.11
Footing elastic rigidity (vertical direction)	K_{NN}	[MN/m]	4247.64	2577.32
Footing elastic rigidity (horizontal direction)	K_{VV}	[MN/m]	3688.98	2193.60
Footing elastic rigidity (rotational direction)	K_{MM}	[MNm]	92178.41	23443.05
Footing dashpot coefficient (vertical direction)	A_{NN}	[MNs/m]	76.26	30.88
Footing dashpot coefficient (horizontal direction)	A_{VV}	[MNs/m]	5.43	2.20
Footing dashpot coefficient (rotation)	A_{MM}	[MNms]	0.00	0.00
Plastic parameter for virgin loading	h_0/K_{NN}	[-]	4.00	4.00
Plastic parameter for reloading	p	[-]	0.50	0.50
Non-associative parameter	p_g	[-]	5.00	5.00
Uplift initiation parameter (strip footing geometry)	α	[-]	4.00	4.00
Uplift parameter	γ	[-]	1.00	1.00
Uplift parameter	δ	[-]	1.00	1.00
Uplift parameter	ε	[-]	0.20	0.20
Uplift - plasticity coupling parameter	ζ	[-]	1.50	1.50

(b)

Table 2: Additional geometric and mechanical parameters of studied bridge pier configurations.

It is interesting to note that the maximum foundation overturning moment is $M_{f,\max} = 133.7$MNm for P30L and only $M_{f,\max} = 34.5$MNm for P30S. Yield bending moment of the pier section is $M_{p,y} = 43.0$MNm for both configurations.

Tables 2(a) and 2(b) provide some additional parameters characterizing the two configurations. In particular, Table 2(b) provides the parameters for the definition of foundation macro-element, following [5] and [7].

4 RECORD SET FOR INCREMENTAL DYNAMIC ANALYSES

The implementation of IDA requires the definition of a concise set of seismic records that correspond to a prescribed earthquake scenario (defined, for example, by the couple {Magnitude, distance} and given geotechnical conditions). The number of records in this set must be large enough to cover uncertainties related to the obtention of a representative acceleration time history in terms of spectral accelerations, strong phase duration, characteristic intensity measures *etc*. In standard IDA applications (*cf*. [6]), calculations are performed for a set comprising at least 30 records. Once such a record set has been defined, uniform scaling is applied to all records to achieve a preselected range of values for one or more characteristic intensity measures. In most cases, scaling is performed with respect to PGA, but other intensity measures can be used, as for example, Arias intensity, CAV *etc*.

Notwithstanding the necessity of a dense record set compatible with a specific earthquake scenario, the following IDA implementations will be performed for a record set comprising 12 signals that have been obtained from different recent earthquakes exhibiting variable characteristics. This record set comes from the studies of Meza & Papageorgiou [3], [4] and, in the present context, offers the advantage that for the selected records, it has been possible to extract the surface wave components in the definition of the translational and rotational ground motions. Consequently, for the two degrees-of-freedom of interest for the presented analyses, three separate signals are provided:

a) total motion q_{tot}, which corresponds to what has been recorded *in situ*
b) extracted motion q_{SW}, which corresponds to the contribution of surface waves in the recorded motion
c) body wave motion q_{BW}, which is the motion exempt of the effect of surface waves ($q_{\text{BW}} = q_{\text{tot}} - q_{\text{SW}}$); it is thus understood that q_{BW} comprises exclusively the effect of body waves

In the above definitions, we use q to designate generically either horizontal translation u or rotation θ about a horizontal axis (rocking). The signals are provided in terms of displacements; velocities and accelerations are obtained by differentiation. The method for extracting the surface wave component of the recorded signals has been exhaustively presented in [13] and [14].

Table 3 presents main properties and intensity measures of the selected records. For each record, we provide the seismic event of origin and some basic features (year, location, magnitude, depth), the time step $\mathrm{d}t$ used for definition of the provided signal and corresponding Nyquist frequency f_{N}. Then, for each of the two retained degrees-of-freedom (translation / rotation), Table 3 provides characteristic intensity measures for total motion q_{tot}, extracted motion q_{SW} and body wave motion q_{BW}, with $q \equiv u$ for horizontal translation and $q \equiv \theta$ for the rocking. The provided intensity measures are: a) maximum acceleration, b) maximum velocity, c) maximum displacement, d) Arias Intensity I_A, e) Cumulative Absolute Velocity CAV and f) effective duration t_f. Definition of I_A, CAV and t_f for rotational motions is extrapolated from corresponding definitions for translations.

The presented IDA analyses are performed for five PGA levels defined with reference to motions u_{BW} : The considered intensity levels are: {0.1g, 0.2g, 0.3g, 0.4g, 0.5g}. All other motions are scaled accordingly so that the above PGA levels are assured for motion u_{BW}. Basic scaling factor as reported in Table 3, is the coefficient that multiplies the initial signal so that PGA of motion u_{BW} becomes equal to 0.1g.

	N/N	[-]	1	2	3	4	5	6	7	8	9	10	11	12
Record	Earthquake	[-]	Niigata-ken Chuetsu	Niigata-ken Chuetsu	Niigata-ken Chuetsu	Niigata-ken Chuetsu	El Mayor-Cucapah	El Mayor-Cucapah	Chi-Chi aftershock 1803	Chi-Chi aftershock 1803	Chi-Chi aftershock 1803	Chi-Chi aftershock 1803	Tohoku	Tohoku
	Year	[-]	2004	2004	2004	2004	2010	2010	1999	1999	1999	1999	2011	2011
	Magnitude	M	6.8	6.8	6.8	6.8	7.2	7.2	6.2	6.2	6.2	6.2	9.0	9.0
	Depth	[km]	300	300	300	300	206.7	206.7	60	60	60	60	29	29
	Record Name	[-]	CHB026	CHB013	SIT011	TKY015	GVDA10	GVDA00	TCU140	TCU145	TCU118	TCU112	TKY020	TKY018
	Time Step	[dt]	6.5096E-02	6.5096E-02	6.6879E-02	6.6879E-02	5.0397E-02	5.0397E-02	3.5073E-02	3.5073E-02	3.1398E-02	3.1398E-02	4.0002E-02	4.0002E-02
	Nyquist frequency	[Hz]	7.68	7.68	7.48	7.48	9.92	9.92	14.26	14.26	15.92	15.92	12.50	12.50
	BASIC SCALING FACTOR		16.68	13.45	3.90	6.76	9.13	6.40	3.18	2.79	2.78	3.95	0.93	0.70
u_{tot} Total Translation	Maximum Acceleration	[m/s2]	0.0600	0.0743	0.2566	0.1477	0.1789	0.1732	0.3624	0.3970	0.4547	0.3559	1.1494	1.7348
	Maximum Velocity	[m/s]	0.0131	0.0136	0.0320	0.0279	0.0349	0.0326	0.1630	0.1419	0.1470	0.1169	0.2516	0.3572
	Maximum Displacement	[m]	0.0123	0.0103	0.0199	0.0227	0.0570	0.0410	0.1322	0.1203	0.1030	0.0891	0.1004	0.1032
	Arias Intensity	[m/s]	0.0022	0.0019	0.0175	0.0134	0.0094	0.0103	0.1097	0.0853	0.0912	0.0613	0.9748	2.0134
	CAV	[m/s]	1.556	0.830	2.686	3.170	1.717	1.666	6.349	5.438	4.631	3.630	23.282	32.197
	Effective Duration	[s]	243.3	87.9	70.2	157.7	46.0	40.8	58.3	62.0	47.8	43.3	103.3	95.4
u_{SW} Extracted Translation	Maximum Acceleration	[m/s2]	0.0153	0.0103	0.0442	0.0415	0.1691	0.0665	0.1486	0.2079	0.1655	0.1691	0.5674	0.7527
	Maximum Velocity	[m/s]	0.0110	0.0065	0.0200	0.0249	0.0321	0.0323	0.1140	0.0811	0.1101	0.0800	0.0688	0.1299
	Maximum Displacement	[m]	0.0100	0.0056	0.0133	0.0228	0.0457	0.0405	0.0883	0.0656	0.0843	0.0694	0.0356	0.0466
	Arias Intensity	[m/s]	0.0002	0.0001	0.0010	0.0012	0.0040	0.0021	0.0297	0.0193	0.0196	0.0185	0.1325	0.4033
	CAV	[m/s]	0.204	0.106	0.376	0.454	0.681	0.623	2.947	2.386	1.952	1.951	8.614	13.342
	Effective Duration	[s]	34.6	17.1	25.8	24.2	17.6	29.4	49.8	53.5	30.9	37.1	128.7	92.3
u_{BW} Translation (without SW)	Maximum Acceleration	[m/s2]	0.0599	0.0743	0.2565	0.1479	0.1096	0.1562	0.3144	0.3587	0.3591	0.2530	1.0730	1.4249
	Maximum Velocity	[m/s]	0.0108	0.0104	0.0315	0.0242	0.0130	0.0127	0.0973	0.0801	0.1076	0.0746	0.2335	0.2860
	Maximum Displacement	[m]	0.0102	0.0087	0.0151	0.0154	0.0232	0.0068	0.0768	0.0738	0.0734	0.0582	0.0980	0.0960
	Arias Intensity	[m/s]	0.0019	0.0018	0.0157	0.0118	0.0045	0.0068	0.0614	0.0505	0.0574	0.0290	0.6896	1.2349
	CAV	[m/s]	1.424	0.778	2.509	2.976	1.360	1.361	4.729	4.062	3.620	2.431	19.011	25.262
	Effective Duration	[s]	261.9	81.1	76.0	170.5	78.4	51.6	61.9	64.5	49.4	50.2	96.9	95.1
θ_{tot} Total Rotation	Maximum Acceleration	[rad/s2]	1.759E-04	1.097E-04	2.478E-04	4.567E-04	3.023E-04	2.523E-04	1.019E-03	5.487E-04	9.246E-04	4.760E-04	2.507E-03	7.042E-03
	Maximum Velocity	[rad/s]	1.322E-05	7.946E-06	1.538E-05	2.587E-05	1.867E-05	2.105E-05	4.359E-05	4.758E-05	7.110E-05	4.613E-05	1.195E-04	2.460E-04
	Maximum Rotation	[rad]	1.013E-05	5.214E-06	3.312E-06	5.409E-06	9.823E-06	1.047E-05	3.174E-05	3.038E-05	2.195E-05	1.680E-05	2.227E-05	2.584E-05
	Arias Intensity	[rad/s]	6.216E-09	5.207E-09	1.927E-08	4.276E-08	1.373E-08	2.055E-08	1.368E-07	1.007E-07	1.854E-07	9.337E-08	2.323E-06	1.562E-05
	CAV	[rad/s]	1.784E-03	1.214E-03	2.314E-03	3.253E-03	1.814E-03	2.096E-03	5.471E-03	4.719E-03	5.284E-03	3.638E-03	3.097E-02	7.194E-02
	Effective Duration	[s]	100.0	77.8	40.1	22.9	29.8	31.2	48.5	81.6	28.7	19.7	56.9	44.8
θ_{SW} Extracted Rotation	Maximum Acceleration	[rad/s2]	1.504E-05	7.080E-06	5.310E-06	6.875E-06	6.595E-06	6.693E-06	8.414E-05	1.587E-04	8.952E-05	8.698E-05	8.859E-05	9.218E-05
	Maximum Velocity	[rad/s]	1.172E-05	5.822E-06	4.043E-06	5.762E-06	7.905E-06	8.148E-06	3.401E-05	3.001E-05	2.434E-05	2.491E-05	3.982E-05	3.399E-05
	Maximum Rotation	[rad]	9.942E-06	4.927E-06	3.141E-06	4.752E-06	9.815E-06	1.031E-05	2.677E-05	2.289E-05	1.336E-05	1.470E-05	1.896E-05	1.574E-05
	Arias Intensity	[rad/s]	1.845E-10	3.993E-11	2.542E-11	3.825E-11	3.598E-11	3.739E-11	4.853E-09	6.305E-09	3.508E-09	2.807E-09	1.543E-08	1.448E-08
	CAV	[rad/s]	2.203E-04	8.719E-05	7.867E-05	8.834E-05	8.262E-05	8.377E-05	1.250E-03	1.318E-03	8.142E-04	7.555E-04	3.736E-03	3.387E-03
	Effective Duration	[s]	23.0	15.2	21.5	17.0	14.3	14.1	57.6	137.5	30.9	37.2	189.1	160.1
θ_{BW} Rotation (without SW)	Maximum Acceleration	[rad/s2]	1.758E-04	1.096E-04	2.475E-04	4.566E-04	3.010E-04	2.513E-04	1.028E-03	5.241E-04	8.587E-04	4.920E-04	2.512E-03	7.055E-03
	Maximum Velocity	[rad/s]	8.059E-06	8.092E-06	1.533E-05	2.587E-05	1.834E-05	2.149E-05	4.466E-05	4.607E-05	6.670E-05	4.836E-05	1.092E-04	2.422E-04
	Maximum Rotation	[rad]	1.831E-06	1.331E-06	3.040E-06	3.085E-06	1.957E-06	2.405E-06	1.968E-05	1.859E-05	1.259E-05	8.066E-06	1.818E-05	1.973E-05
	Arias Intensity	[rad/s]	6.023E-09	5.163E-09	1.925E-08	4.271E-08	1.369E-08	2.051E-08	1.289E-07	9.291E-08	1.787E-07	8.948E-08	2.306E-06	1.560E-05
	CAV	[rad/s]	1.688E-03	1.170E-03	2.303E-03	3.239E-03	1.805E-03	2.091E-03	5.089E-03	4.180E-03	5.141E-03	3.415E-03	2.968E-02	7.128E-02
	Effective Duration	[s]	67.0	67.6	40.0	22.7	29.7	31.1	36.6	77.7	28.8	18.0	54.7	44.7

Table 3: Record set for IDA: Intensity measures for translational and rotational components

Some additional comments deserve to be noted for the selected records:

- Motion u_{BW} is used as reference motion for scaling: this is the motion that would be felt by the structure if no effect of surface waves were to be considered for the translational component and if rocking (θ_{BW}) were to be neglected following Biot's principle. Incidence of surface waves will modify the horizontal motion from u_{BW} to u_{tot} ; moreover, it will induce the amplified rotational motion θ_{tot} (with respect to θ_{BW})
- The effective durations, especially for motion u_{tot}, are particularly large, with values that may exceed 4min at least for one record (CHB026: $t_f = 243$s). This is because emphasis is to be given in the surface wave component, which is characterized by low frequencies (below 1Hz) that tend to increase duration if several cycles are contained in the signal

- Accordingly, time step $\mathrm{d}t$ used for the definition of signals is rather large (ranging between 40msec and 70msec, with corresponding Nyquist frequencies f_{N} ranging between 7.5Hz and 16Hz). This implies that high-frequency content is poorly described in the signals but this is a deliberate choice for reducing the number of time steps and, accordingly, computational cost
- Total rotations θ_{tot} in the selected signals are rather limited and this is line with Biot's principle, which postulates quasi-negligible rocking motions. For example, record CHB026 presents $\max\{\theta_{\mathrm{tot}}\} \approx$ 1e^{-05}rad, which after scaling for the highest intensity level ($\max\{\ddot{u}_{\mathrm{BW}}\}$ = 0.5g) yields: $\max\{\theta_{\mathrm{tot}}\} = 5\times16.68\times1\mathrm{e}^{-05}$rad = 0.8mrad. This value corresponds to an imposed drift at the base of the pylon of only 0.8‰.

Figure 2 presents the response spectra of the 12 signals for motions u_{BW}, u_{tot} and θ_{tot} after scaling of u_{BW} to 0.1g. Characteristic frequencies of u_{BW} motions are contained between 0.5Hz and 4Hz. For u_{tot}, this interval increases from 0.2Hz to 4Hz with higher spectral accelerations, especially for the first characteristic peak of the spectrum. Characteristic frequencies for total rotations are between 2Hz and 8Hz. Finally, it is interesting to note that, although all u_{BW} motions are scaled at 0.1g, PGA values for u_{tot} may range from 0.1g to 0.15g, the difference highlighting the increase in PGA due to the surface wave component.

It is recalled that IDA analyses are performed for three hierarchical motion scenarios:

- Scenario 1: Only horizontal translation u_{BW} is applied at the pylon base
- Scenario 2: Only horizontal translation u_{tot} is applied at the pylon base - scenario 2 adds the translation surface wave effect with respect to scenario 1
- Scenario 3: Horizontal translation u_{tot} and rotation θ_{tot} are applied at the base - scenario 3 adds the total rotational effect with respect to scenario 2

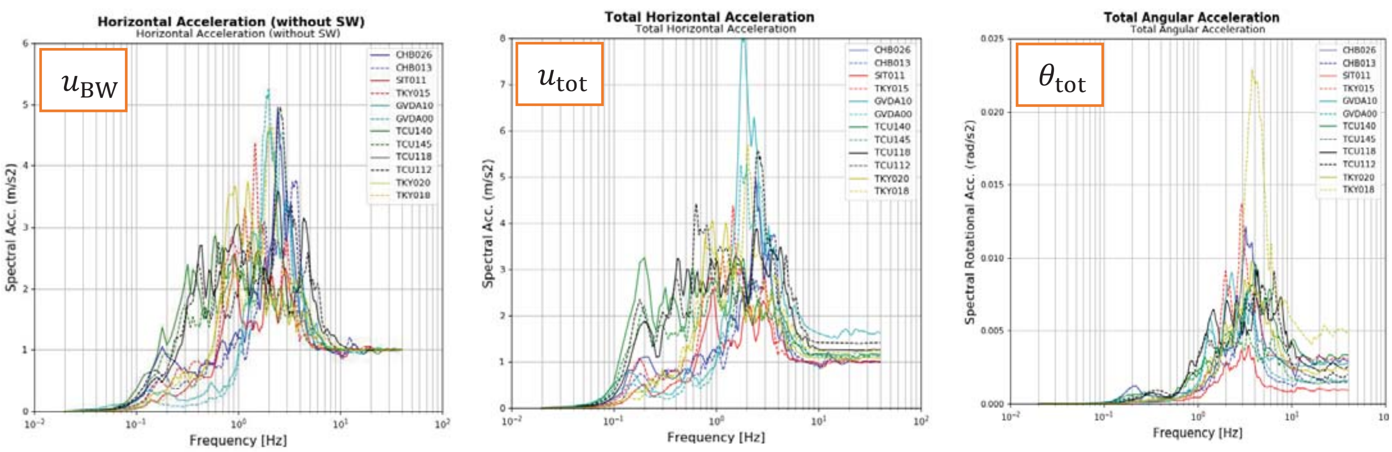

(a) (b) (c)

Figure 2: Record set for IDA: (a) Response spectra of horizontal translations without SW (motion u_{BW}) scaled at 1m/s², (b) Response spectra of total horizontal translations (motion u_{tot}), (c) Response spectra of total rotations (motion θ_{tot})

5 IMPLEMENTATION AND RESULTS

5.1 Organization of computations and results

The computations required for IDA analyses are performed with open-source FEM platform Code_ASTER [8]. The total number of performed analyses is N = 2 pylon configurations × 3 excitation scenarios × 12 records × 5 intensity measures = 360 nonlinear analyses. The calculations are performed in time domain under the assumption of small displacements.

IDA analyses give rise to so-called IDA curves, which present the evolution of a given damage measure (DM) or performance criterion as function of a preselected intensity measure. Following [5], seven damage measures (DM) are used for producing IDA curves and probing the performance of bridge pylon in nonlinear range. The selected DMs are (acronyms are provided in parentheses):

1. Maximum total drift of the deck (MTD) that is obtained from the sum of three components: horizontal displacement of the foundation, foundation rotation and structural drift due to pier deformation
2. Maximum structural drift of the deck (MSD); this is the component of deck displacement which is due exclusively to pier deformation
3. Residual total drift of the deck (RTD); this is deck displacement obtained at the end of excitation. Assuming that pylon vibration has been completed at the end of nonlinear analysis, RTD corresponds to the irreversible components due to sliding and permanent rotation at the foundation and also due to permanent structural drift of the pier
4. Residual structural drift of the deck (RSD), which can be high if the pier response is strongly nonlinear
5. Maximum ductility demand (DD) obtained at the base of the pylon, defined as:

$$\mathrm{DD} = \max\left\{1;\ \frac{\kappa(t)}{\kappa_y}\right\} \tag{4}$$

   where $\kappa(t)$ the developed curvature at the pylon base and κ_y the yield curvature, corresponding to the first exceedance of yield stress in the outer fiber of pier section. If DD = 1, the response is elastic
6. Maximum moment (MM) developed at the base of the pier
7. Accumulated foundation settlement (FS) at the end of loading. Pronounced FS is an indicator of a bearing failure at the foundation, eventually combined with significant permanent rotation

The provided Damage Measures characterize the global behavior and allow identifying significant nonlinear response at the pier or at the foundation. Global parameters are MTD and RTD. Parameters pertaining to the superstructure are MSD, RSD, DD and MM. Finally, FS is an indicator of damage level at the foundation. In what regards the definition of intensity measures, we provide the IDA curve set pertaining to the basic IM used for scaling, which is PGA of motion u_{BW}.

5.2 IDA curves for global DMs

Figures 3 and 4 present the obtained IDA curves for the two global DMs, namely maximum total drift (MTD) and residual total drift (RTD) of bridge deck. For presentation of IDA curves, the same figure setup is always adopted. Each presented figure contains two plots: in the left side, results for P30S (small foundation) are plotted, in the right side for P30L (large foundation). IDA curves are plotted in space {DM, IM}, where horizontal axis corresponds to the studied DM and vertical axis to the selected IM, which is PGA of u_{BW} varying from 0.1g to 0.5g. Each plot contains the following data:

- The raw data from transient analyses corresponding to 3 scenarios, 5 intensity levels and 12 records. These data are plotted as grey circles; each plot contains 180 data points;
- For each excitation scenario, a statistical treatment allows plotting the median value together with 16% and 84% percentiles of studied DM as function of increasing IM. Median values are presented with continuous lines, percentiles are presented with dotted lines. Each excitation scenario is represented by a specific color. Scenario 1 (excitation with u_{BW}) is represented in blue; scenario 2 (excitation with u_{tot}) is represented in green;

scenario 3 (excitation with u_{tot} and θ_{tot}) is represented in red. In the following we may refer to scenario 1 as SC1 (respectively for 2 and 3). SC2-3 will indicate scenarios 2 and 3 together.

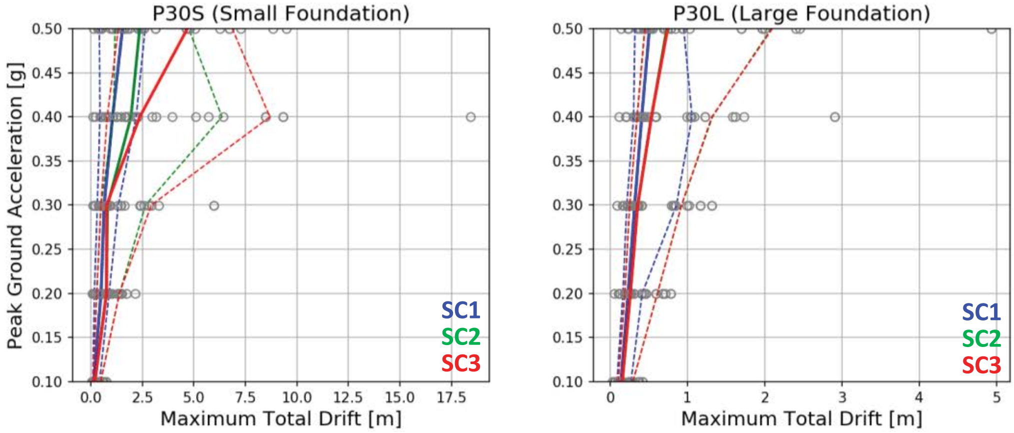

Figure 3: IDA curve for global parameter MTD (Maximum total drift)

IDA curves for global parameter MTD, as presented on Figure 3, indicate a sharp contrast in response for the two studied configurations. For P30S, maximal MTD can be as high as 17.5m for the most critical data point. Despite the fact that this is an isolated value, it certainly indicates development of a bearing failure mechanism at foundation level, accompanied by pronounced rotations. For P30L, maximal MTD is 5m and this is due to nonlinear pier response in bending. For P30S, median curves are all increasing with increasing IM and it is interesting to note that up to 0.30g, there is little difference between SC1 and SC2-3. Beyond 0.3g however, the difference between the three scenarios is more pronounced and one can notice an initial increase from SC1 to SC2, then an additional distress when passing to SC3. This indicates that both the total rotational component and the translational component of surface waves can have an impact on the response for very strong events, in case of yielding foundation systems. On the contrary, in P30L, median curves show a slight increase in MTD when passing from SC1 to SC2, but no additional distress when passing to SC3. Actually, SC3 curves are strictly superimposed to SC2 curves, implying that the consideration of θ_{tot} has no impact on the final result even for very high intensities. Finally, the extent of percentile curves is an indicator of variability in response. In P30S, SC2-3 present clearly larger variabilities than SC1 and this is due to highly nonlinear foundation response. For P30L, there is still a difference in variability between SC1 and SC2-3, but it is less pronounced.

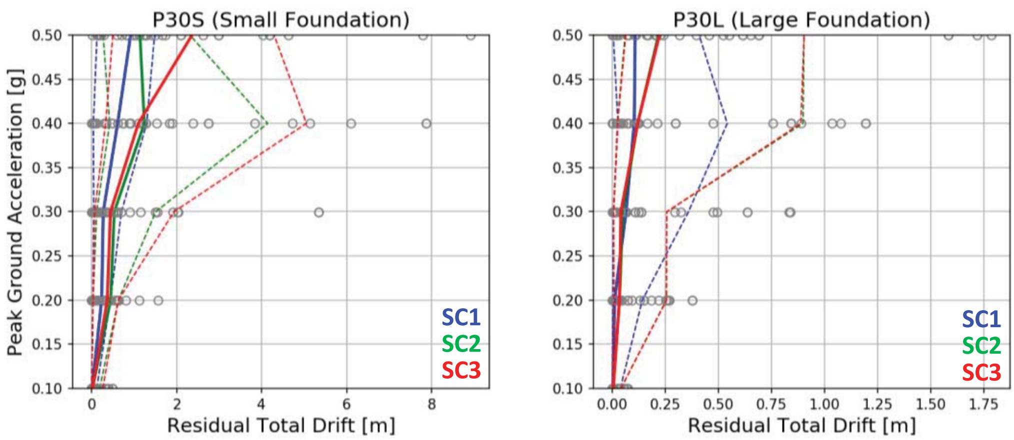

Figure 4: IDA curve for global parameter RTD (Residual total drift)

Figure 4 presents the obtained IDA curves for residual total drift (RTD). Again, the performance of P30S is much more critical than for P30L. The maximal obtained RTD value for P30S can be as high as 8m or more for a very strong earthquake and obviously this corresponds to a failure at foundation level that leads to non-tolerable residual displacements at bridge deck. In terms of mean values, it is interesting to note that SC1 leads to RTDs that increase slightly with intensity and remain less than 1m even at 0.50g. When the effect of surface waves is considered (SC2-3), RTD may be increased by factor 2 or more with respect to SC1. Rocking component (SC3) can lead to even higher RTD values for very strong events.

RTD evolution for P30L seems to remain independent of considered scenario for intensities up to 0.40g. It is needed to reach 0.50g to see a difference between SC1 and SC2-3. As for MTD, SC2-3 are strictly superimposed (both median and percentile curves are almost identical).

5.3 IDA curves for structural DMs

Figures 5 to 8 present IDA curves for four DMs pertaining to the response of the pier, namely maximum structural drift (MSD), residual structural drift (RSD), ductility demand at pylon base (DD) and maximum developed bending moment at the base (MM). All four DMs are clear indicators of the "isolation effect" offered by the reduced foundation design in P30S as compared to P30L.

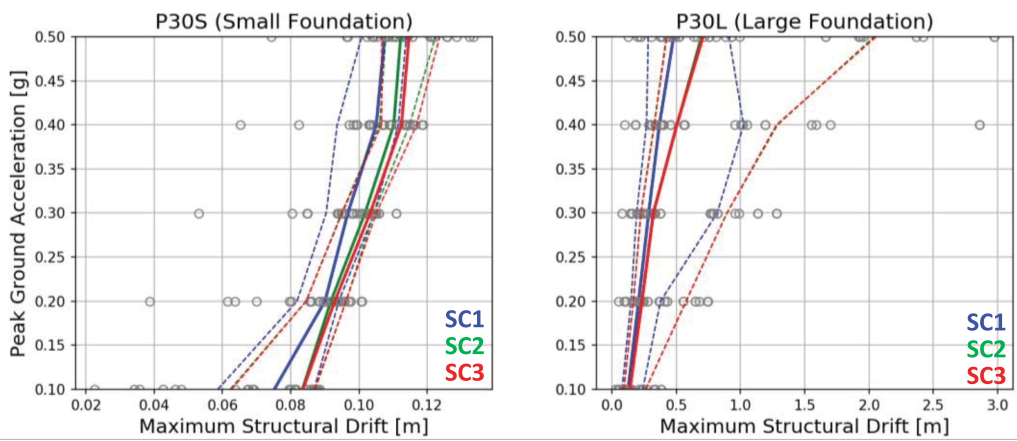

Figure 5: IDA curve for structural parameter MSD (Maximum Structural Drift)

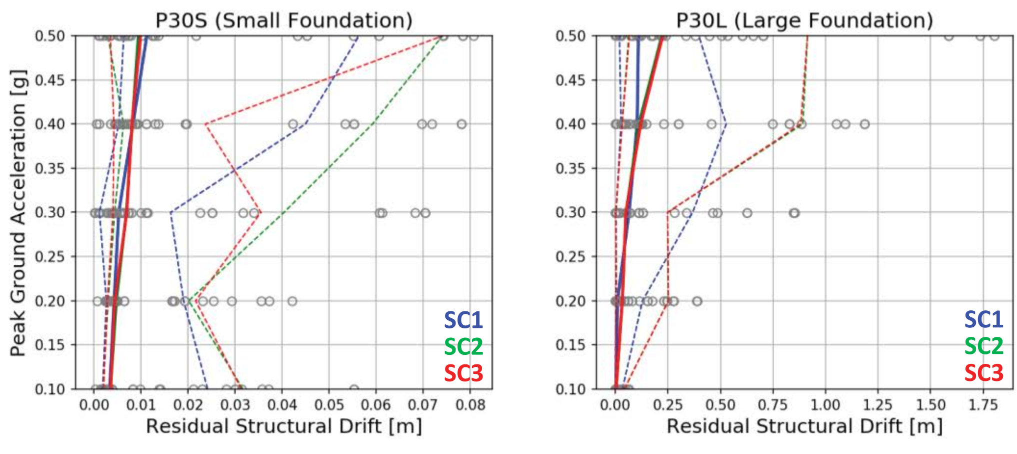

Figure 6: IDA curve for structural parameter RSD (Residual Structural Drift)

More specifically, Figure 5 presents IDA curves for maximum structural drift (MSD). For P30S, MSD values are limited, not exceeding 15cm for the most severe case in the data set. On the contrary, MSD values for P30L can be as high as 3m (isolated data point). In terms of influence of surface waves, MSD increases slightly from SC1 to SC2 and then to SC3 for P30S for all intensities beyond 0.2g. In the case of P30L, SC2-3 are strictly superimposed (both median and percentile curves). The passage from SC1 to SC2 leads to an increase in distress, which is amplified as intensity increases.

Figure 6 presents IDA curves for residual structural drift (RSD). It is recalled that residual values are the ones obtained at the end of transient analysis and it is supposed that pylon vibration has been completed. For P30S, median RSD values on Figure 6 are less than 1cm and present significant variability: these values are actually "spurious" and originate from the fact that pylon vibration has not been perfectly dissipated by the final time step in transient analyses; if the analyses were to be continued further, RSD curves for P30S would be excepted to fall identically to zero. Results for P30L are almost identical to the results for RTD presented on Figure 4. This implies that RTD in case of P30L is only obtained from the structural component while the foundation contribution is negligible (as expected, since the foundation response is quasi-linear).

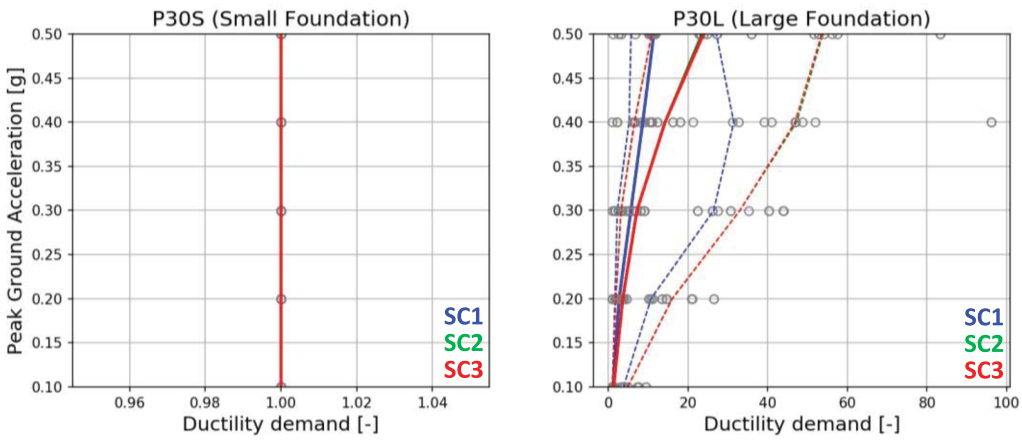

Figure 7: IDA curve for structural parameter DD (Ductility Demand at pier base)

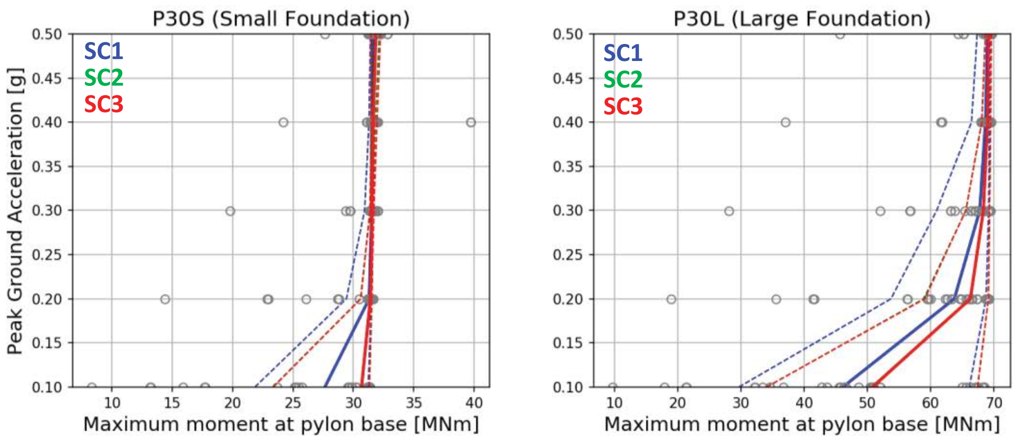

Figure 8: IDA curve for structural parameter MM (Maximum bending moment at pier base)

Figure 7 presents IDA curves for ductility demand (DD) at the pylon base. The result for P30S is very clear: all DDs are strictly equal to 1, which means that the pylon response remains elastic for all intensity levels. This a clear manifestation of the "capacity-design" approach, which guides all damage to a structural element (here, the foundation) and thus protects another structural element (here, the pier). In case of P30L, "capacity-design" is inversed. Consequently, median DD curves at the pylon base are quickly raising with intensity level and may reach the value 10 for SC1 at 0.5g. The effect of surface waves increases even further median DD values, exceeding the value 20 at 0.5g. As in the previous cases for P30L, SC2-3 are superimposed: the effect of surface waves comes from the translational component. The rotational component induces no further distress on the system.

Figure 8 presents the obtained IDA curves for maximum bending moment developed at the pylon base (MM). An interesting feature of these curves is that, contrary to the previously examined DMs, here the variability is larger for smaller intensities. As IM is increased, IDA curves (both median and percentiles) tend asymptotically to a characteristic value. For P30S, this value is 34.5MNm (*cf.* Table 2b) and corresponds to the foundation overturning moment capacity. For P30L, this value is almost 70MNm and corresponds to the bending moment capacity of the pier. Recall, that for P30L, the overturning capacity at the foundation is 133.7 MNm (*cf.* Table 2b).

5.4 IDA curve for DMs pertaining to foundation response

As a final result, Figure 9 presents IDA curves for foundation settlement (FS), which is a performance indicator of foundation response. As expected, response for P30L is very favorable, with median settlements not exceeding 2cm for the strongest intensity level. The effect of surface waves is almost negligible and median curves for SC1 and SC2-3 are almost superimposed. On the contrary, the performance for P30S is -as expected- much more severe. Median settlements for SC1 are 0.25m at 0.5g but exhibit very high variability. Corresponding 84% percentile value is at least 4 times larger (>1.0m). The effect of surface waves almost doubles median FS for high intensities and one can observe a slight additional distress in passing from SC2 to SC3.

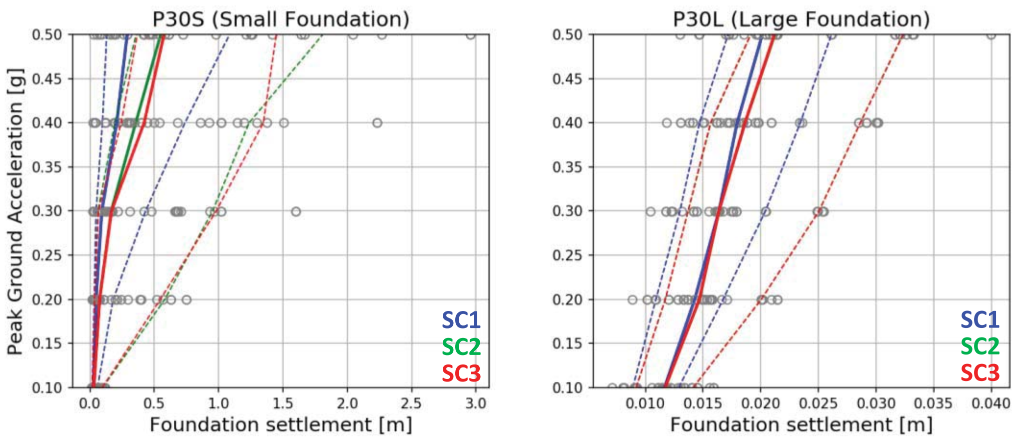

Figure 9: IDA curve for foundation parameter FS (accumulated Foundation Settlement)

6 CONCLUSIONS AND PERSPECTIVES

The present work has focused on the assessment of detrimental effects that surface waves may induce on bridge pylons. Two pylon configurations were studied, with emphasis on two variants for foundation design: a) conventional design, in which the foundation exhibits overstrength with respect to bridge pylon base section, b) inversed capacity-design, in which foundation dimension is reduced so as to concentrate nonlinear response at the foundation and thus protect the superstructure. The pylons have been studied via the IDA technique using a set of twelve records, in which it has been possible to isolate the effect of surface waves for horizontal translation and rocking. Basic conclusions of the study are the following:

- The detrimental effect of surface waves is mainly due to the horizontal motion component, at least for the record set used in this study. Even so, the effect of surface waves may lead to a significant increase in demand for both studied configurations. For the pylon with yielding superstructure, ductility demands at the pylon base section may be doubled due to surface waves. For the pylon with yielding foundation, foundation settlements may equally be doubled because of surface waves
- Detrimental effects of surface waves become more severe as seismic intensities increase. For seismic levels up to 0.20g, the response seems to be slightly altered by the incidence of surface waves
- An observable effect of the rocking motions has only been obtained for very high intensities and only for the configuration with yielding foundation. In the case of yielding superstructure, rocking motions have induced no further damage with respect to horizontal translations
- Bridge pylons designed with yielding foundations remain an interesting option for seismic design as a means for avoiding excessive damage in the superstructure. However, these systems seem to be more vulnerable to the effect of surface waves than conventional systems.

The presented results constitute the preliminary step for a detailed assessment of the effect of surface waves on bridge pylons within the framework or French research project ANR MODULATE. Prospective research works can focus on the following topics:

- A parametric investigation of a large number of pylon configurations (exploiting the proposed surrogate) model and confrontation with real cases
- Further IDA analyses and construction of fragility curves for record sets enriched with new records. As a matter of fact, one of the main objectives of the research project is to generate such records, both from post-processing of natural recordings and by large-scale numerical computations in realistic and canonical subsoil topographies. A further understanding is required as to the influence of rocking motions and as to how large rocking motions (induced by surface waves) can be. IDA analyses can further be investigated as to the selection of most relevant damage and intensity measures for the studied problem
- Last but not least, the studies can be extended to analyses for large displacements, which is a more rigorous hypothesis for systems near instability, foundation failure or extensive structural damage. Another possible extension is towards more realistic modeling of mechanical behavior in the concrete pier. Some selected pylon configurations can become the object of detailed 3D analyses.

7 ACKNOWLEDGEMENTS

This research work has received funding from the French National Research Project ANR MODULATE (2018 - 2022). More details and updates on ANR MODULATE can be accessed through the project website: https://modulate.brgm.fr.

REFERENCES

[1] Biot MA (1933): Theory of elastic systems vibrating under transient impulse with an application to earthquake-proof buildings. Proc Natl Acad Sci 1933; 19(2); 262-268

[2] Trifunac MD (2009): The role of strong motion rotations in the response of structures near earthquake faults. Soil Dynamics and Earthquake Engineering, 29 (2009); 382-393

[3] Meza Fajardo KC, Papageorgiou AS (2018): Response of tall buildings to base rocking induced by Rayleigh waves. Earthquake Engineering & Structural Dynamics, 2018; 47:1755-1773, https://doi.org/10.1002/eqe.3040.

[4] Meza Fajardo KC, Papageorgiou AS (2019): Ductility demands of tall buildings subjected to base rocking induced by Rayleigh waves. Earthquake Engineering & Structural Dynamics, 2019; 1-21, https://doi.org/10.1002/eqe.3179.

[5] Chatzigogos CT, Meza Fajardo KC, Papageorgiou AS (2020): Nonlinear response of bridge pylons to surface wave passage. Proceedings of 17WCEE, Sendai, Japan, September 13-18, 2020

[6] Vamvatsikos D, Cornell CA (2002): Incremental Dynamic analysis. Earthquake Engineering and Structural Dynamics, 31:491-514

[7] Chatzigogos CT, Figini R, Pecker A, Salençon J (2011): A macroelement formulation for shallow foundations on cohesive and frictional soil. International Journal for Numerical and Analytical Methods in Geomechanics, 2011; 35: 902-931

[8] Code_ASTER - Analyse des Structures et Thermo-Mécanique pour des Etudes et des Recherches (https://www.code-aster.org)

[9] Gazetas G (1991): Foundation vibrations. In Foundation Engineering Handbook, Chapter 15, Fang HY(ed.), Van Nostrand Reinhold, NY.

[10] Dafalias YF, Hermann LR (1982): Bounding surface formulation of soil plasticity. In Soil Mechanics - transient and cyclic loading, Pande GN, Zienkiewicz PC (eds.), Wiley, pp. 173-218.

[11] Chatzigogos CT, Pecker A (2009): Project DARE - Soil-Foundation-Structure systems beyond conventional seismic failure thresholds, GDS Internal report 32-09_N1A.

[12] Anastasopoulos I, Gazetas G, Loli M, Apostolou M, Gerolymos N (2010): Soil failure can be used for seismic protections of structures. Bulletin of Earthquake Engineering, 8:309-326

[13] Meza Fajardo KC, Papageorgiou AS (2016): Estimation of rocking and torsion associated with surface waves extracted from recorded motions. Soil Dynamics and Earthquake Engineering, 2016; 80:225-240

[14] Meza Fajardo KC, Papageorgiou AS, Semblat JF (2015): Identification and extraction of surface waves from three - component seismograms based on the normalized inner product. Bulletin of Seismological of America 2015; 105(1):210-229